

Laser beam shaping limitations for laboratory simulation of turbulence using a phase-only spatial light modulator

Igor A. Litvin^{1,2}, Liesl Burger^{1,3}, Mapula P. De Gama^{1,3}, Ally Mathye^{1,3} and Andrew Forbes^{1,3†}

¹CSIR National Laser Centre, PO Box 395, Pretoria 0001, South Africa

²Laser Research Institute, University of Stellenbosch, Stellenbosch 7602, South Africa

³School of Physics, University of Kwazulu–Natal, Private Bag X54001, Durban 4000, South Africa

ABSTRACT

Recent approaches to demonstrating adaptive optics and atmospheric turbulence have made use of spatial light modulators (SLMs) as the active phase element. However, there are limitations in using SLMs as an accurate method of simulating turbulence phase screens. In this work we investigate the limitation of laser beam shaping with a phase-only spatial light modulator for the simulation of dynamic and pseudo-random turbulence in the laboratory. We find that there are regimes where there are not sufficient pixels to resolve the phase. At the higher end of this range, at strong turbulence levels, the zonal regions are tightly packed. This leads to two simultaneous effects: a phase screen with low efficiency in some regions, and a modified turbulence structure due to the shifting of the zone peaks. These amplitude and phase distortions have a deleterious effect on the accurate simulation of the turbulence. At the lower end of the range, at weak turbulence, the phase change is too small to describe with sufficient grey scale levels, since the full 256 levels are associated with a full 2π phase shift. Further limitations include the frame rate of SLM for time-evolving turbulence. We show experimental results demonstrating these limitations, and discuss the impact this has on simulating turbulence with SLMs.

Keywords: Kolmogorov turbulence, spatial light modulator, diffraction, binary optics

1. INTRODUCTION

The use of adaptive optics for atmospheric turbulence correction is fairly commonplace these days in both astronomical and military applications (see refs. [1] and [2] for a good overview of the field). The use of spatial light modulators (SLMs) (or their early variants) have previously been suggested and used for the production of Zernike modes, adaptive optics and turbulence generation^{3–7}. Most of the approaches attempting to demonstrate turbulence have concentrated on Kolmogorov turbulence, and have made use of the SLM as the turbulence screen. The studies have concentrated on the impact of the turbulence on the laser beam and the use of SLMs as closed-loop correctors of turbulence.

In this paper we have two basic aims: firstly, to expound on the steps required to actually simulate atmospheric turbulence in the laboratory, and secondly, to point out some of the limitations in using spatial light modulators as turbulence simulators from a laser beam shaping perspective. That is to say, we are not so much interested in the turbulence itself but the impact of the SLM in simulating this turbulence. We will consider Kolmogorov turbulence as an example, and describe the effects of a single phase screen on the far field intensity pattern of a laser beam. In section 2 we will review the theory needed to create simple turbulence phase screens, and show how to implement these in a laboratory setting in section 3. Finally, in section 4, we highlight some limitations of using a spatial light modulator for this application.

2. CREATING KOLMOGOROV PHASE SCREENS

There are a few simple steps required to calculate a phase screen that describes turbulence. Firstly, one must select a turbulence model to use. Here we select Kolmogorov turbulence as an example, which is valid within the inner and outer scales. With this selection, one is left with the requirement that the turbulence model chosen should somehow

† Corresponding author: Andrew Forbes; tel: +27 12 841 2368; fax: +27 12 841 3152; email: aforbes1@csir.co.za

relate to the method used to describe the phase. The Zernike polynomials form a neat basis set for describing optical phase with the convenient properties that: (a) the polynomial coefficients can be directly related to the known optical aberrations, (b) the polynomials are complete and orthogonal, and (c) the polynomial coefficients required to describe Kolmogorov turbulence can be calculated analytically. We first introduce the polynomials, and then show how they are linked to our choice of turbulence model.

2.1 Zernike basis set

The phase screen was calculated by decomposing the phase function into a series of Zernike polynomials, and thus an understanding of these polynomials is important. The Zernike polynomials are a set of orthogonal polynomials that arise in the expansion of a wavefront function for optical systems with circular pupils. If we assume that the pupil is of unit radius, then the expansion of an arbitrary function $\phi(\rho, \theta)$ where $\rho \in [0,1]$ and $\theta \in [0,2\pi]$, in an infinite series of these polynomials will be complete. The circle polynomials of Zernike have the form of complex angular function modulated by a real radial polynomial:

$$Z_n^m(\rho, \theta) = \sqrt{2(n+1)} R_n^m(\rho) e^{im\theta}, \quad (1)$$

where $n \geq |m|$, $n \geq 0$ and $n - m = \text{even}$.

It can be shown that the radial function also obeys an orthogonality relation, and is given by:

$$R_n^m(\rho) = \sum_{k=0}^{\frac{n-m}{2}} \frac{(-1)^k (n-k)!}{k! \left(\frac{n+m}{2} - k\right)! \left(\frac{n-m}{2} - k\right)!} \rho^{n-2k}. \quad (2)$$

The radial function is normalised such that $R_n^m(1) = 1$. By definition, $R_n^m = 0$ when $n - m \neq \text{even}$. Equation (1) can be written as

$$Z_n^m(\rho, \theta) = \sqrt{2(n+1)} R_n^m(\rho) [\cos(m\theta) + i \sin(m\theta)], \quad (3)$$

thus we can construct two real functions U_n^m and V_n^m such that

$$Z_n^m(\rho, \theta) = U_{nm}(\rho, \theta) + i V_{nm}(\rho, \theta), \quad (4)$$

and

$$\phi(\rho, \theta) = \sum_{n=0}^{\infty} \sum_{m=0}^n [A_{nm} U_{nm}(\rho, \theta) + B_{nm} V_{nm}(\rho, \theta)]. \quad (5)$$

Since the phase is completely described by the sum of the terms in (5), we need only calculate the coefficient terms for Kolmogorov turbulence in order to create the desired phase screen.

2.2 Noll matrix

Kolmogorov turbulence screens can be created by calculating the spatial covariance matrix from the Zernike expansion of the phase, following the approach of Noll⁸. The resulting matrix, I_{nm} (the so-called Noll Matrix), can be used to calculate the statistical nature of the Zernike coefficients needed to describe Kolmogorov turbulence. In particular, if it is assumed that the Zernike coefficients are normally distributed with mean zero, then the variance of the distribution is found from the diagonal terms of the Noll Matrix and can be expressed as:

$$\sigma_{nm}^2 = I_{nm} \left(\frac{D}{r_0} \right)^{5/3}, \quad (6)$$

with

$$I_{nm} = \frac{0.15337(-1)^{n-m}(n+1)\Gamma(14/3)\Gamma(n-5/6)}{\Gamma(17/6)^2\Gamma(n+23/6)}. \quad (7)$$

The parameter r_0 is the turbulence coherence length, or Fried's scale parameter, and D is the diameter of the aperture (in this case the phase screen diameter). Fried's parameter is determined by the model used for C_n^2 and is given by:

$$r_0 = \left[0.423k^2 \int_{h_{\min}}^{h_{\max}} C_n^2(h)dh \right]^{-5/3}, \quad (8)$$

where h is the height from some reference level, usually ground or sea level. The key parameter in the turbulence model is the refractive index structure constant, C_n^2 , which in general is a function of altitude, and is a measure of the turbulence strength.

For example, in order to calculate the value of the A_{20} coefficient in (5), one simply draws a random number from a normal distribution with mean zero and variance given by (6). Since all the coefficients are now easily calculated, the summation in (5) can readily be accomplished, thus building a Kolmogorov phase screen.

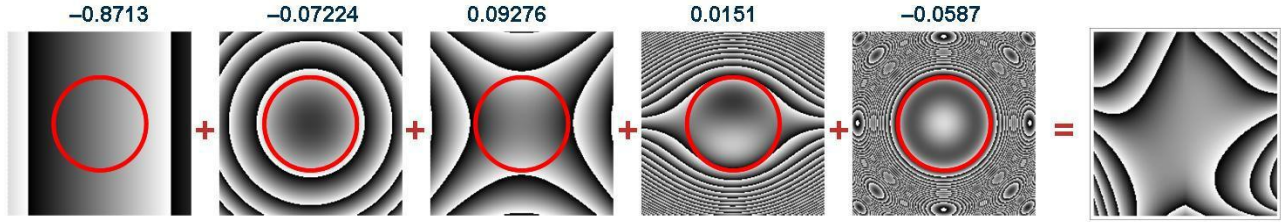


Figure 1: The row of images shows, from left to right, five of the Zernike polynomials representing tilt, defocus, coma, astigmatism and spherical aberration respectively. When each is weighted by the factor given above the plots (random numbers), the summed result is the turbulent phase screen on the far right. The red circles indicate the unit circle over which the polynomials are valid.

2.3 Time varying turbulence

The easiest method of creating a time varying turbulence phase is to make use of the successive samples from the random sequence just described, build multiple phase screens from these samples, and then "play" the phase screens one after the other to simulate a time varying turbulence screen. A more rigorous method is that put forward by Voitsekhovich⁹, which allows for the generation of dynamic phase screens based on the covariance of the refractive index function that includes both spatial and temporal statistics:

$$B_l(\tau) = 12.32(n+1)D^{-2}r_0^{-5/3} \int_0^\infty x^{-1} J_{n+1}^2(x) \Phi(2x/D) \left[J_0\left(\frac{2v\tau}{D}x\right) + (-1)^{l+m}(1-\delta_{0m})J_{2m}\left(\frac{2v\tau}{D}x\right)\cos(2m\theta) \right] dx, \quad (9)$$

where θ is the wind direction and v the wind speed. Each polynomial l then has an associated temporal covariance function, from which the mean square of the Zernike coefficients, which represent the spatial characteristics, can be deduced by setting $\tau = 0$. The power spectral density for Kolmogorov turbulence is defined as:

$$\Phi_n(\kappa) = 0.033C_n^2\kappa^{11/3}. \quad (10)$$

Equations (9) and (10) allow both the temporal and spatial changes to be described, thus dynamic turbulent phase screens can be generated.

3. LABORATORY DEMONSTRATION

Phase screens were calculated according to the procedures discussed in the previous section, and digitised into a 256 level grey scale image, representing a 0 to 2π phase shift on our phase-only spatial light modulator (Holoeye, model 1080P). The spatial light modulator (SLM) was illuminated with a Gaussian beam, expanded from a Helium Neon laser so as to have a near flat wavefront at the SLM. Far field intensity patterns were generated using a Fourier transforming lens, and captured with a CCD camera (Cohu, model 4812). A schematic of the set-up is shown in Figure 2.

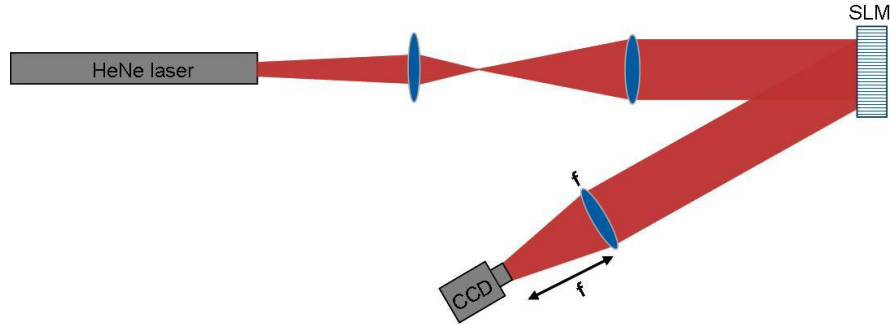


Figure 2: Schematic of the experimental arrangement. A HeNe laser beam is delivered with a near flat wavefront at the SLM, which then imparts the turbulence phase screen on the beam. The far field intensity is measured by placing the CCD camera at the focal plane of a lens.

There are two main components to the far field intensity pattern: a beam wandering effect due to the tip/tilt phase contributions, and a beam intensity change due to the influence of higher order terms on the phase structure. These higher order terms lead to larger beams, and in some cases scintillation. The full effects of turbulence are described in Figure 3. The sequence of images from (a) – (d) show experimental images of decreasing levels of turbulence with associated phase screens. As expected, the beam returns back to a near Gaussian intensity when the turbulence is weak.

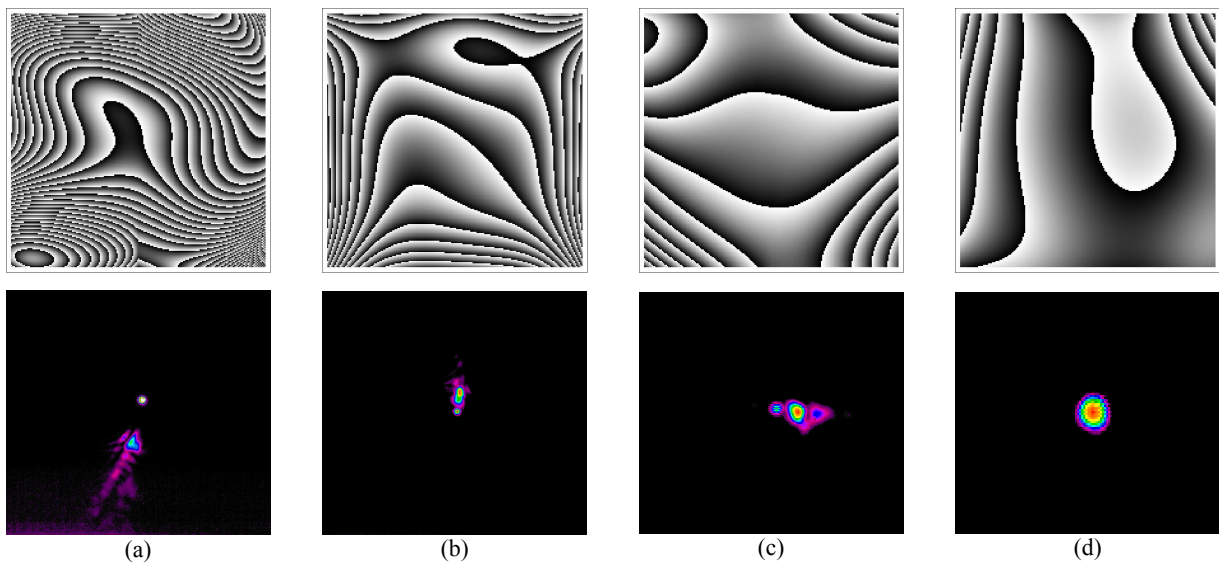


Figure 3: Examples of turbulence phase screens (top row) in order of decreasing turbulence from (a) to (d), with the resulting (measured) laser beam intensity change shown below the respective screen.

In Figure 3 (a) the zero order is clearly seen as a central bright spot. Since the experimental images are captured after a Fourier transforming configuration, one can readily calculate the expected intensity distribution at the camera for comparison between theory and experiment. In the far field the phase modulation due to the Kolmogorov screen is fully

realized as intensity changes (this would not be the case had the intensity been measured immediately after the phase screen). Figure 4 show a sequence of images: (a) the input Gaussian beam at the SLM, (b) an example phase screen written to the SLM, (c) the calculated laser beam intensity at the camera and (d) the measured laser beam intensity at the camera.

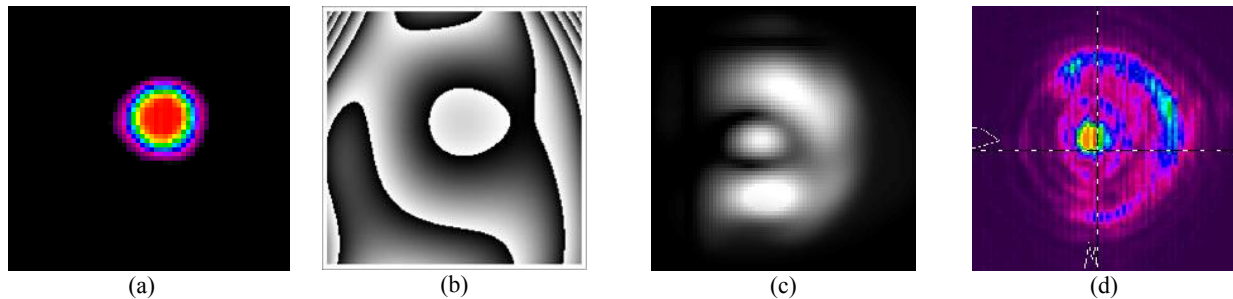


Figure 4: (a) Gaussian input, (b) digital phase screen written to SLM, (c) calculated far field intensity and (d) measured far field intensity.

There is good agreement between the calculated and measured laser beam intensities, with both showing a bright central spot surrounded by a semi-circle of light. Calculations for Figure 4 were based on $D = 5.7$ mm and $r_0 = 0.001$ m.

4. SPATIAL LIGHT MODULATOR LIMITATIONS

In addition to demonstrating laboratory-based turbulence, we have also explored the limitations of using phase-only SLMs for this application. While this analysis is generally true for *all* SLMs, we highlight the issues by using our SLM as an example. The stated features of the SLM are:

- 1920 x 1080 pixels (8 μ m pitch),
- 8 bit encoding (256 levels),
- 60 Hz refresh rate,
- 60% of intensity in 0th order.

We find that although the SLM is very versatile in simulating turbulence, there are regimes where it is not well suited due to insufficient resolution to resolve the phase element. For very strong turbulence the zonal regions are tightly packed. This is evident in Figure 5 (a), where near the edges of the phase screen the modulation in phase is very rapid, and cannot be resolved sufficiently by the available pixels on the SLM. This leads to two simultaneous effects: a variable level binary element with low efficiency at some points, thus changing the amplitude transmission, and a modified turbulence structure due to shifting in the zone peaks (since the zone positions determine the function of the element) as a result of poorly resolved phase transitions.

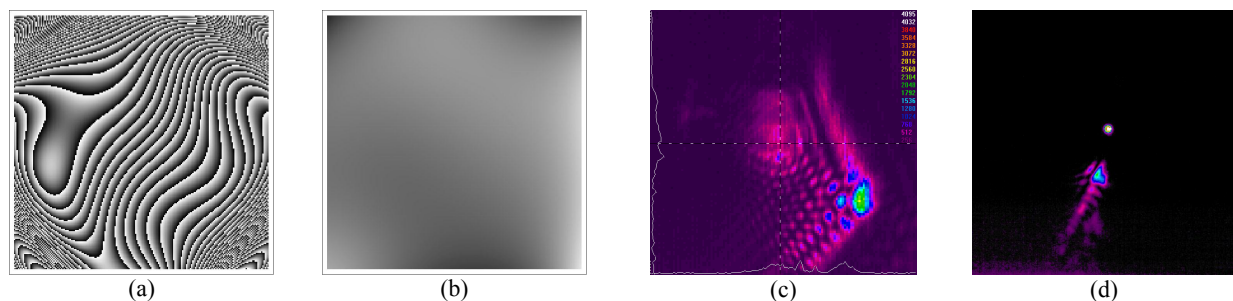


Figure 5: (a) Very strong turbulence phase screen; (b) very weak turbulence phase screen; (c) – (d) examples of measured far field intensity profiles.

At the lower end of the range the phase change (Figure 5 (b)) is too small to describe with sufficient grey scale levels, since the full 256 levels is associated with a 2π phase shift. Thus again the continuous phase function is written as a low level binary element. The implications of these deleterious effects can be seen in Figures 5 (c) and (d): in the former,

the additional energy in the various diffraction orders, due to the binary effects of SLM resolution, are noticeable; in the latter case, the zeroth order is very evident indicating the low diffraction efficiency of the SLM under these conditions (the reader is warned however that Figures 5 (a) and (c) do not form a pair, and likewise with (b) and (d)). Further limitations include the frame rate of the SLM for time evolving turbulence, placing restrictions on the input parameters to the model, such as wind speed.

In order to quantify some of the effects noted above, consider that the efficiency of the SLM in producing the desired turbulence output in the m^{th} order is given by:

$$\eta = \left[\frac{\sin(\pi m / N)}{\pi m / N} \right]^2, \quad (11)$$

with the energy distributed in discrete orders given by $m = pN + 1$ (for integer p), with N the number of pixels used in describing the phase between zones. Figure 6 shows a strong turbulence screen with example cross-sections showing the phase modulation ($0-2\pi$) and the corresponding zones. The figure highlights that the zone spacing is not uniform across the SLM, and in this case the spacing between zones decreases towards the edges of the SLM.

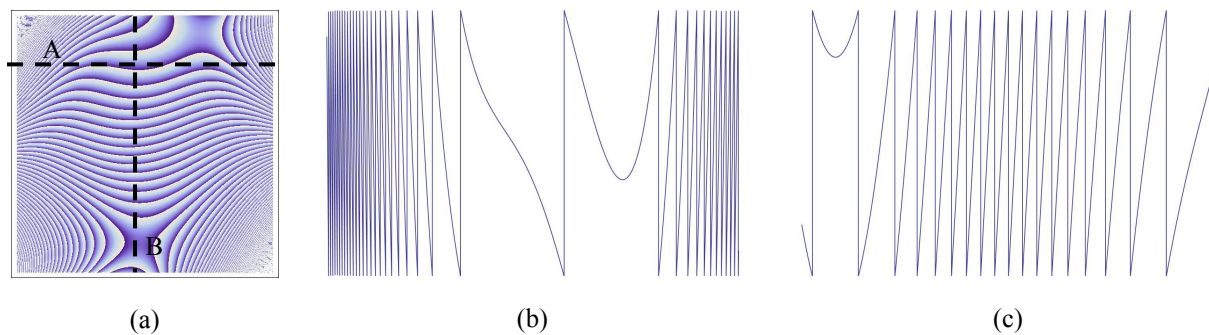


Figure 6: (a) Example of a strong turbulence screen ($D = 5.7$ mm and $r_0 = 0.001$ m) with two cross-section lines, (b) example horizontal cross-section (A) of the phase, (c) example vertical cross-section (B) of the phase.

To illustrate the impact of this, we calculate the effective efficiency of the phase screens of Figure 6 (b) and (c) as written to the SLM, assuming for convenience that the phase screens are written across 1000 pixels. The results are shown graphically in Figure 7 (a) and (b) respectively.

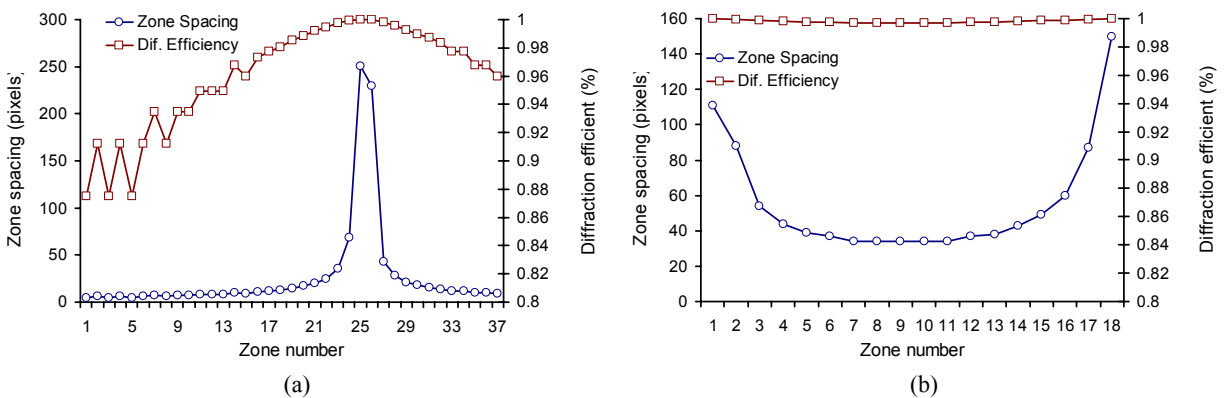


Figure 7: Impact of SLM pixel limitations on resolving the zones in the generated phase screens: (a) shows the results using Figure 6 (b) as an input, while (b) shows the results using Figure 6 (c) as an input.

In the horizontal cross-section (Figure 7 (a)) the zone spacing is limited to only a few pixels near the edge, which decreases the efficiency in the 1st order to roughly 88%. The varying efficiency across the element leads to an effective amplitude mask which needs to be included in all calculations. In contrast, Figure 7 (b) shows high efficiency across

the entire phase screen due to the large zone spacing. Note that these calculations are based on the phases shown in Figure 6 (b) and (c), which we treated as independent functions in this analysis in order to better illustrate the SLM limitation. When the turbulence is increased further, with $D = 5.7$ mm and $r_0 = 0.0001$ m, the SLM is reduced to single pixel representation of each zone, thus resulting in either zero diffraction efficiency or zone shifting in a two level element – both undesirable.

When the turbulence is weak ($D = 5.7$ mm and $r_0 = 0.1$ m) the SLM is still capable of resolving the small phase changes with roughly 5 pixels, giving >80% efficiency. As the turbulence is decreased further still, so the number of pixels used decreases until the SLM displays a single phase change across the entire beam in the limit of very weak turbulence.

5. CONCLUSION

In this work we have outlined the basic steps required in order to simulate atmospheric turbulence in the laboratory with a spatial light modulator. We have highlighted some of the issues with using SLMs for this application, and discussed the impact this has on the actual phase screen written to the SLM, which shows binary grating-like problems.

REFERENCES

1. L.C. Andrews and R.L. Phillips, "Laser beam propagation through random media", SPIE Optical Engineering Press, 1998.
2. L.C. Andrews, "Field guide to atmospheric optics", SPIE Optical Engineering Press, 2004.
3. G.D. Love *et al*, "Binary adaptive optics: atmospheric wavefront correction with a half-wave phase shifter", *Appl. Opt.*, vol. 34, pp. 6058 – 6066, 1995.
4. G.D. Love *et al*, "Intensity-only modulation for atmospheric scintillation correction by liquid-crystal spatial light modulators", *Opt. Lett.*, vol. 21, pp. 1496 – 1498, 1996.
5. G.D. Love, "Wavefront correction and production of Zernike modes with a liquid crystal spatial light modulator", *Appl. Opt.*, vol. 36, pp. 1517 – 1524, 1997.
6. G.T. Bold *et al*, "Practical issues for the use of spatial light modulators in adaptive optics", *Opt. Comm.*, vol. 148, pp. 323 – 330, 1998.
7. D.C. Dayton *et al*, "Theory and laboratory demonstrations on the use of a nematic liquid crystal phase modulator for controlled turbulence generation and adaptive optics", *Appl. Optics*, vol. 37, pp. 5579 – 5589, 1998.
8. R.J. Noll, "Zernike polynomials and atmospheric turbulence", *J. Opt. Soc. Am.*, vol. 63 (3), pp. 207-211, 1976.
9. V. V. Voitsekhovich, "Outer scale turbulence: comparison of different models", *J. Opt. Soc. Am. A* vol. 12 (6), pp. 1346–1353, 1995.